Biochemistry **1996,** *35,* 83−88

Interpretation of Transient-State Kinetic Isotope Effects[†]

Harvey F. Fisher* and Swapan K. Saha*

Department of Biochemistry, University of Kansas Medical Center, and Department of Veterans Affairs Medical Center, Kansas City, Missouri 64128

Received April 24, 1995; Revised Manuscript Received September 8, 1995[⊗]

ABSTRACT: In contrast to steady-state kinetic isotope effects (KIE's), transient-state KIE's are dependent on both time and signal source. We developed a theory which predicts the behavior of transient-state KIE's, permits the calculation of the intrinsic KIE, and makes possible the assignment of various optical signals to either pre- or post-hydride transfer events. We proved that the behavior of KIE$_{obs}$ for a reversible two-step reaction for all possible values of the rate constants and all possible ratios of intermediate and product contributions obeys three simple rules (assuming that the isotope-sensitive step involves a hydride transfer): (1) If only the post-hydride species contributes to the observed signal, KIE$_{obs}$ = KIE$_{int}$ at $t = 0$ and then decreases with time. (2) If only the pre-hydride species contributes to the observed signal, then KIE$_{obs}$ = 1 at $t = 0$ and then decreases with time. (3) If both pre- and post-hydride species contribute to the observed signal, then KIE$_{obs}$ = 1 at $t = 0$ and then will either rise or fall with time depending on the relative molar signal coefficients of the pre- and post-hydride species. We provide experimental evidence that the phenomena predicted by this theory do in fact occur in enzyme-catalyzed reactions.

Kinetic isotope effects (KIE's) have been widely used for two distinguishable but related purposes: The determination of the intrinsic KIE (KIE$_{int}$) provides information about the nature of the transition involved in a specific bond-breaking step, while, even in cases where KIE$_{int}$ cannot be determined, the examination of observed KIE's (KIE$_{obs}$) constitutes a powerful set of tools for deducing changes in rate-limiting steps in complex reactions and for locating rate-limiting steps in their reaction sequences. The applications of this approach have been particularly fruitful in the study of enzyme reactions. Nearly all of the work in this area has involved the steady-state kinetic approach, and a substantial body of sophisticated theory has been developed for the interpretation of the results of such experiments.

Relatively little attention has been paid to the study of transient-state kinetic isotope effects. Melander and Sanders have pointed out the difficulties that arise in the interpretation of KIE$_{obs}$ in even the simplest of reactions involving a reversible step (Melander & Sanders, 1980). Only a handful of transient-state kinetic studies of enzyme-catalyzed reactions have been reported, possibly due to the lack of any suitable theory applicable to such data.

Theoretical Development. Cleland has developed a very elegant theory which expresses the effect of post-hydride transfer related rate constants on KIE$_{obs}$ determined from the relative rates of the pre-steady-state burst (Cleland, 1989). While this theoretical treatment does provide a further degree of mechanistic dissection, it does not utilize the early nonlinear portion of the transient phenomena which frequently dominate such time courses. We present here a theory which does provide a means of understanding both the events which precede the isotope-sensitive step as well as those which follow it.

We will consider the reaction:

$$\mathrm{A} \underset{k_2}{\overset{k_1}{\rightleftharpoons}} \mathrm{B} \underset{k_4}{\overset{k_3}{\rightleftharpoons}} \mathrm{C} \tag{1}$$

where k_3 and k_4 designate the isotope-sensitive steps. The general analytical solution for the system shown in Figure 1 is well-known (Moore & Pearson, 1981).

$$\begin{gathered} p = k_1 + k_2 + k_3 + k_4 \\ q = \sqrt{p^2 - 4(k_1k_3 + k_2k_4 + k_1k_4)} \\ \lambda_2 = \frac{1}{2}(p + q) \qquad \lambda_3 = \frac{1}{2}(p - q) \end{gathered} \tag{2}$$

It can be shown that for the unsubstituted reaction

$$[\mathrm{B}](t) = k_1\left(\frac{k_4}{\lambda_2\lambda_3} + \frac{k_4 - \lambda_2}{\lambda_3(\lambda_2 - \lambda_3)}\right)e^{-\lambda_2 t} + k_1\frac{\lambda_3 - k_4}{\lambda_3(\lambda_2 - \lambda_3)}e^{-\lambda_3 t} \tag{3}$$

$$[\mathrm{C}](t) = k_1k_3\left[\frac{1}{\lambda_2\lambda_3} + \frac{e^{-\lambda_2 t}}{\lambda_2(\lambda_2 - \lambda_3)} - \frac{e^{-\lambda_3 t}}{\lambda_3(\lambda_2 - \lambda_3)}\right] \tag{4}$$

where [B] and [C] represent the molar concentrations of components B and C of eq 1.

Corresponding equations can be written for the isotopically labeled reaction by substituting k_3/KIE$_{int}$ for k^{D}_3 and k_4/KIE$_{int}$ for k^{D}_4.

If the measured signal $s(t)$ consists of contributions from two product species whose molar absorbance (or fluorescence) coefficients are b and c, then the values of the observed signal at any given time for the unsubstituted reaction (s^{H}) and for the isotopically substituted reaction (s^{D})

[†] This work was supported in part by Grant MCB-922119 from the National Science Foundation, Grant GM-47108 from the General Medicine Institute of the National Institutes of Health, and the Department of Veterans Affairs.

* Correspondence should be addressed as follows: Research Service, VA Medical Center, 4801 Linwood Blvd., Kansas City, MO 64128. Telephone (816) 861-4700 X7156; FAX (816) 861-1110.

[⊗] Abstract published in *Advance ACS Abstracts,* December 15, 1995.

0006-2960/96/0435-83$12.00/0

are given by eqs 5 and 6, respectively.

$$s^{\mathrm{H}}(t) = b[\mathrm{B}] + c[\mathrm{C}] \tag{5}$$

$$s^{\mathrm{D}}(t) = b[\mathrm{B_D}] + c[\mathrm{C_D}] \tag{6}$$

By inserting the time dependences of [B] and [C] from eqs 3 and 4 into eq 5, we obtain an equation which expresses the time dependence of the observed signal s^{H}, and by making the same substitutions in eq 6, we obtain the corresponding equation for s^{D}. The resulting equations are quite straightforward, but when written out in their fully expanded form, they are far too large to write out in full here. We will therefore use the expressions $s^{\mathrm{H}}(t)$ and $s^{\mathrm{D}}(t)$ with the understanding that exact solutions to the full time dependences of these two parameters can be calculated for the system described in eq 1, for any given values of k_1, k_2, k_3, k_4, b, and c.

A steady-state $\mathrm{KIE_{obs}} = v_{\mathrm{H}}/v_{\mathrm{D}}$, where v_{H} and v_{D} represent the initial steady-state reaction rates of the unsubstituted and the substituted reactions, respectively. Since $v = c[\mathrm{C}]$, where [C] is the concentration of the product and c is the signal coefficient of that product, a steady-state isotope effect is defined as

$$\mathrm{KIE_{obs}} = \frac{\mathrm{d}([\mathrm{C_H}])/\mathrm{d}t}{\mathrm{d}([\mathrm{C_D}])/\mathrm{d}t} \tag{7}$$

By analogy (albeit not a perfect one), we now extend this definition to include a time dependence using $s^{\mathrm{H}}(t)$ and $s^{\mathrm{D}}(t)$ from eqs 5 and 6.

$$\mathrm{KIE_{obs}}(t) = \frac{\mathrm{d}[s^{\mathrm{H}}]/\mathrm{d}t}{\mathrm{d}[s^{\mathrm{D}}]/\mathrm{d}t} \tag{8}$$

We will use this definition of a transient-state KIE in the treatment that follows here and in the accompanying paper (Maniscalco et al., 1996).

Calculation of Theoretical Transient-State KIE_{obs} Time Courses. Since, as we have pointed out, the values of s^{H} and of s^{D} can be calculated arithmetically by simply assigning finite values to the four rate constants in eq 4 and designating a specific time, t, by assigning specific values to signal coefficients a and b in eq 5, and by assuming a given value of $\mathrm{KIE_{int}}$ to generate eq 6, it is clear that the time courses of $s^{\mathrm{H}}(t)$ and $s^{\mathrm{D}}(t)$ could, in principle, be calculated manually. We have used the Mathcad 3.1 program (MathSoft, Inc.) run on a PC 486 for this purpose.

While eqs 2−6 can be solved with nothing more than arithmetic and exponentiation, eqs 7 and 8 require the calculation of the derivatives of the time courses expressed by eq 5, and Mathcad 3.1 carries out this calculation by an interactive numerical calculation using Ridder's algorithm and does so with a single key stroke without any perceptible delay. The theoretical curves presented below were calculated in this manner. Each represents such calculations for about 100 sequential values of t, which is sufficient to provide an apparently solid curve. (Other programs, such as Sigma Plot, can also carry out these same calculations, varying only slightly in speed and convenience.)

General Dependence of $\mathrm{KIE_{obs}}$ on Time and on the Specific Signal Observed. In panel A of Figure 1 we compare the time course of a reaction in which no isotopic substitution has been made in the original species A with that of the same reaction where a deuterium atom has replaced a protium atom in each reactive bond position. (These curves were generated using eqs 5 and 6, respectively.) The time courses where both the pre- and post-hydride transfer steps contribute equally to the signal being observed are indicated by the curves designated as $b = 1$. The isotopically substituted and unsubstituted time courses for the same reaction, where only the final product species C contributes to the signal, are indicated by the curves designated as $b = 0$. Panel B of Figure 1 shows the time courses of the $\mathrm{KIE_{obs}}$ (calculated by eq 8) for the reaction as measured by each of the two different signals. *It is clear that $\mathrm{KIE_{obs}}$ is dependent both on time and on the nature of the signal by which the reaction is followed.*

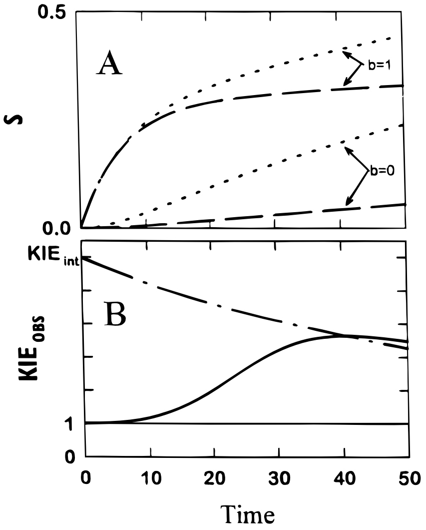

FIGURE 1: Dependence of $\mathrm{KIE_{obs}}$ on time and on the nature of the signal observed. Panel A: time courses of a two-step reversible reaction where the second step is isotopically sensitive. Time courses for the isotopically substituted (− −) and for the corresponding nonisotopically substituted reaction (···), assuming $\mathrm{KIE_{int}} = 6$, $k_1 = 45$, $k_2 = 107$, $k_3 = 28$, and $k_4 = 7.5$ as defined in eq 1. The traces designated $b = 1$ assume that both species B and C contribute to the signal, while the pair designated $b = 0$ assume that only species C is being observed (see eq 7). Panel B: Dependence of $\mathrm{KIE_{obs}}$ vs time calculated from the time courses shown in panel A. The $b = 0$ case is indicated by (− · −) and the $b = 1$ case by (—). $\mathrm{KIE_{int}} = 6$ has been assumed for pictorial purposes in panel B of this figure and Figures 2 and 3, but the qualitative conclusions portrayed hold true for any value of $\mathrm{KIE_{int}} > 1$.

Analysis of the Dependence of $\mathrm{KIE_{obs}}$ on Time and on the Relative Contributions of Individual Species to the Signal. We can divide the entire field of behavior of $\mathrm{KIE_{obs}}$'s that can arise from a reaction described by eq 1 (assuming that k_3 and k_4 represent hydride transfer steps) into three cases: case I, where the signal observed arises *solely* from the final product C; case II, where the signal observed arises *solely* from the intermediate B; and case III, where both pre- and post-hydride transfer species B and C contribute to the signal. We will consider each case in turn.

Case I (Only Post-Hydride Step Species Observed). The time courses of the corresponding deuterated and protiated reactions for a typical case of this class ($k_1 = k_2 = k_3 = k_4$, $b = 0$, $c = 1$, and $\mathrm{KIE_{int}} = 6$) are shown in Figure 2A. The $\mathrm{KIE_{obs}}$ time courses for the series of such reactions where the value for each individual k is lowered sequentially by a factor of 10 are shown in Figure 2B. It can be seen that,

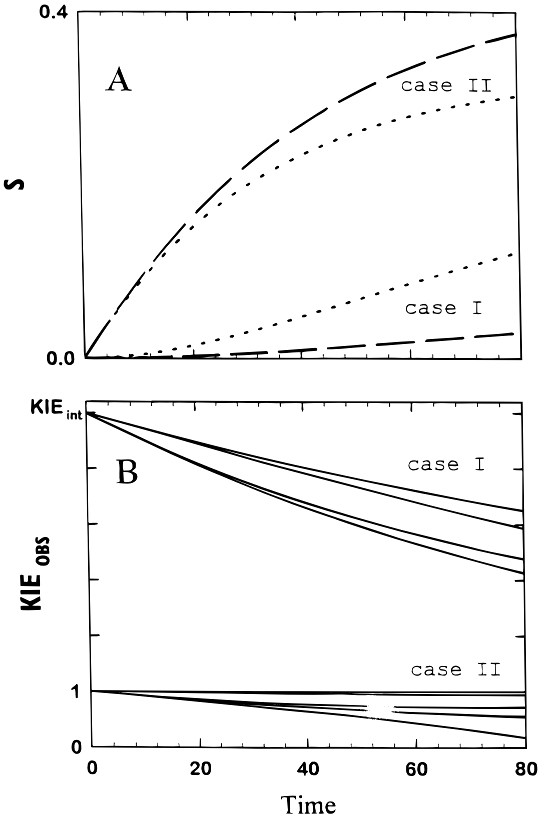

FIGURE 2: Panel A: typical time courses for the same reaction where $k_1 = k_2 = k_3 = k_4 = 10\ s^{-1}$. Cases I and II are those in which *only* species C contributes to the signal and in which *only* species B contributes, as described in the text. Isotopic designations are as described under Figure 1. Panel B: KIE_{obs} time dependences for the same reaction, where each single rate constant has been decreased by a factor of 10 in successive traces. The specific rate constants varied are (from top to bottom) k_4, k_3, k_1, k_2 (and none) for case I and k_3, k_1, k_2 (and none), k_4 for case II.

regardless of which step is rate limiting, $KIE_{obs} = KIE_{int}$ at $t = 0$ and then decreases with time. We have explored a wide variety of values and combinations of values of the individual rate constants and have found no exception to this conclusion.

Case II (Only Pre-Hydride Step Species Observed). The time courses of the corresponding deuterated and protiated time courses for a typical case of this class (again, with all rate constants equal but where $b = 1$ and $c = 0$) are shown in Figure 2A. The KIE_{obs} time courses for the series of such reactions where the value for each individual k is lowered sequentially by a factor of 10 are shown in Figure 2B. It can be seen that, regardless of which step is rate limiting, $KIE_{obs} = 1$ at $t = 0$ and then decreases with time. Again, various combinations of widely varying individual rate constants show no exception to this conclusion.

Case III (Both Pre- and Post-Hydride Step Species Observed). Figure 3A shows the time course of the corresponding deuterated and protiated time courses for a typical case of this class (again, rate constants are all equal). Figure 3B shows the KIE_{obs} time courses for a series of such reactions where the b/c ratio (the relative contributions of pre- and post-hydride species to the signal) is systematically varied. It can be seen that, regardless of which step is rate limiting, $KIE_{obs} = 1$ at $t = 0$ and then either increases with time to a maximum value and then decreases or decreases to a minimum value depending only on which species makes the greatest contribution to the signal. Again, we have found no exceptions to this conclusion.

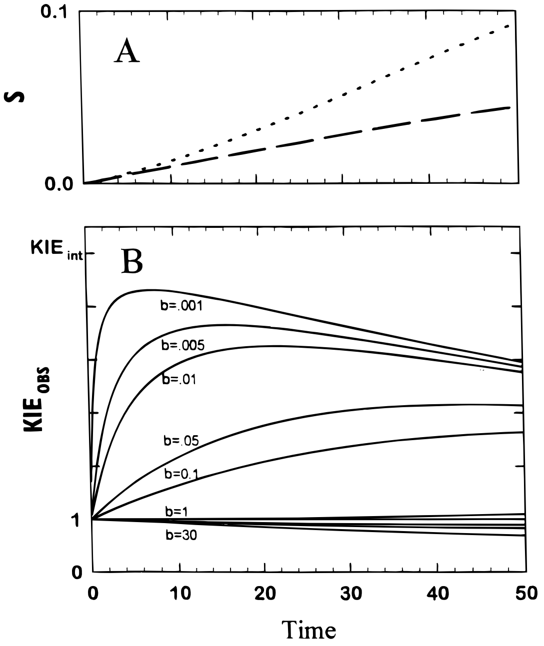

FIGURE 3: Panel A: typical time courses for the same reaction in the case where both species B and C contribute to the signal (isotopic designations are as described under Figure 1). Panel B: KIE time dependences for the same case where $c = 1$ and b varies as indicated (eq 7). The curves (and those in Figures 2 and 3) were generated by entering eqs 3−7 and 9 into a Mathcad program which then calculated exact solutions for the required parameters at successive time intervals of 0, 01. The program calculated the necessary first derivative functions by a variation of Ridder's numerical method.

Thus, we can summarize the behavior of KIE_{obs} for a reversible two-step reaction for all possible values of the rate constants and all possible ratios of intermediate and product contributions with the following three simple rules:

(1) If only the post-hydride species contributes to the observed signal, $KIE_{obs} = KIE_{int}$ at $t = 0$ and then decreases with time.

(2) If only the pre-hydride species contributes to the observed signal, then $KIE_{obs} = 1$ at $t = 0$ and then decreases with time.

(3) If both pre- and post-hydride species contribute to the observed signal, then $KIE_{obs} = 1$ at $t = 0$ and then will either rise or fall with time depending on the relative molar signal coefficients of the pre- and post-hydride species.

These conclusions can be extended to more complex reaction schemes. If the first step in eq 1 is designated as the isotope-sensitive step, so that there is one pre-hydride and two post-hydride species, the three rules stated above still apply rigorously; any contributions from the second product species add only a further increment to the time-dependent decrease of KIE_{obs}. Numerical integration of Laplace transform equations for the extended reaction

$$A \rightleftharpoons B \rightleftharpoons C \rightleftharpoons D$$

where the $B \rightleftharpoons C$ step is assumed to be isotopically sensitive, followed by application of eqs 7 and 8, does not reveal any violations of the three rules listed above, and they must therefore be assumed to be valid for a linear reaction scheme of any number of steps. It is also apparent from the KIE time courses shown that even a very small pre-hydride species contribution causes the KIE_{obs} to have the value of 1 at $t = 0$, but if the signal coefficient of that species is less than 1% of the post-hydride species, then the early exponential portion of the descending time course may be extrapolated back to $t = 0$, to yield the KIE_{int}, a value not otherwise obtained even in a system of this limited degree of complexity. Furthermore, although we have assumed an equilibrium $KIE_{int} = 1$, the conclusions described above are valid even where this assumption does not hold. It is also important to note that conclusions 1, 2, and 3 are valid even in cases where the two isotope-sensitive rate constants are 2 orders of magnitude larger than any rate limiting constant in the reaction.

There are several additional points of interest relating to the KIE_{obs} vs time functions. It can be seen from eqs 2−4 that all four rate constants appear in each term of the expressions for both [B](*t*) and [C](*t*). It follows, therefore, that an isotopic step can cause a KIE_{obs} effect even on signals which arise from specific species not directly involved in such a step. It is also necessary to note in this connection an important difference between steady-state and transient state KIE_{obs}'s. From the mathematical assumptions which define the steady state, the isotopically substituted and unsubstituted reactions are both essentially in the same state. Their complement of the various species and the concentrations of those species remain the same, during the time of measurement. Therefore, a steady-state KIE_{obs} must be independent of time and independent of the signal by which the reaction rate is measured. These statements apply to transient-state reactions only under two conditions: (1) at $t = 0$ and (2) whenever a local steady state occurs. Cleland (1989) used just such a local feature in applying a steady-state analysis to the data we had reported (Fisher et al., 1970). However, it has been our subsequent experience that the occurrence of such local steady states is in fact rather rare. Quite to the contrary, in the transient state the effect of the isotopic step is to alter the time course so that the two reactions become out of phase with each other, and this displacement generally becomes more pronounced with time. Indeed, Cleland pointed out that isotopic substitution could induce a lag phase in a transient time course which did not occur in its absence. As a result of this progressive phase displacement, KIE_{obs} time courses can exhibit dramatic phenomena at sufficiently long times. Such late-occurring effects are quite trivial and can be easily understood by simply observing the relationship between the individual time courses. The rates of the multiexponential increases or decreases in KIE_{obs} are of such extreme complexity that no obvious physical significance can be obtained from their resolution and analysis beyond the conclusions we have already stated.

Experimental Examples of the Theory. In this section we provide evidence that the occurrence of all three cases of KIE_{obs} vs time behavior predicted in the foregoing theoretical section can, in fact, be experimentally demonstrated. The reaction employed for cases I and III is the oxidative deamination of α-deuterio- and α-protio-L-glutamate catalyzed by bovine liver glutamate dehydrogenase. The isotopically sensitive step in this reaction is the reversible transfer of a hydride ion from the α-amino carbon atom of L-glutamate to the C-4 carbon atom of the nicotinamide moiety of NADP.

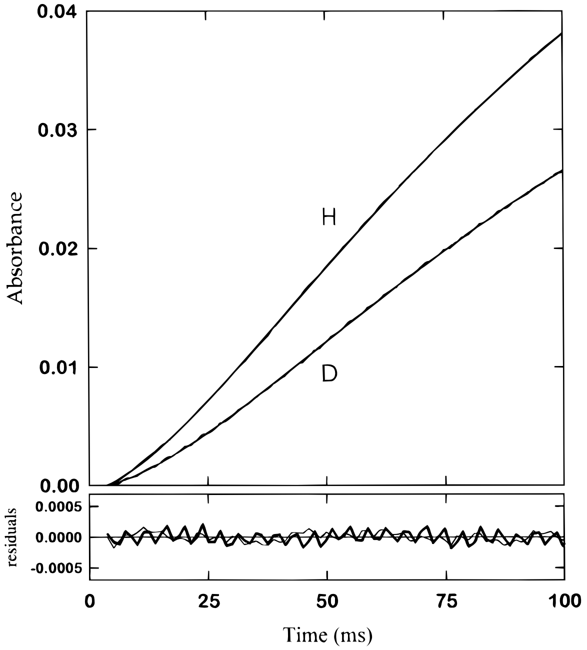

FIGURE 4: Upper panel: the thin lines are the experimentally measured transient-state time courses as measured by 340 nm absorbance for the oxidative deamination of [α-^{1}H]-L-glutamate (labeled H in the figure) and of [α-^{2}H]-L-glutamate (labeled D in the figure) catalyzed by bovine liver glutamate dehydrogenase. The zero time absorbance intercepts have been subtracted from each curve. The reaction conditions are 380 μM NADP, 45 μM enzyme, and 45 mM L-glutamate in 0.1 M phosphate buffer, pH 6.8, 10 °C. Each curve represents the average of 20−30 individual stopped-flow traces. The thick lines indicate the best fit of an arbitrary exponential function and serve only to smooth the data and to provide a differentiable mathematical function, as described in the text. Lower Panel: the deviations between the averaged data and the fitted curve, shown on an expanded scale. The lighter of the two lines in the panel indicates the deviations for the H curve; the heaver line indicates those from the D curve.

The time traces of the 340 nm absorbance signal for the unsubstituted (H) and α-deuterio-L-glutamate (D) reactions are shown by the thin lines in the upper panel of Figure 4. Each line represents the average of 20−30 individual measurements.[1] The definition of $KIE_{obs}(t)$ given in eq 8 requires the calculation of the first derivatives of each of these time courses. We have found that the smoothing of the data by fitting to an arbitrary but explicit mathematical function whose first derivative can be easily calculated by any of a number of readily available computer programs (such as Sigma Plot) is preferable to direct numerical differentiation of such an inherently noisy signal. Any of a number of functions (such as a multiterm polynomial, a cubic-spline function, Gaussians, or exponential functions) can be used. It is important to note that the parameters obtained from such a fit are physically meaningless and are

---

[1] The extrapolated zero-time intercepts of each of the signal time courses shown in Figures 4−6 have been subtracted from the data, thus "pinning" the starting points of each pair of H and D curves to permit easier visual comparison. We have also eliminated the data for the first 7 ms in each case to avoid the small omnipresent early flow anomalies that would otherwise complicate the curve-fitting procedure. Neither of these adjustments have any effect on $KIE_{obs}(t)$. That function, by its nature, reflects only the effects of changes in the concentrations of complexes which are occurring at a given time, *t*, and is completely independent of previous events. The validity of this point is proved by the mathematical operation of taking the first derivative of the fitted functions in eq 8, a step which renders all such constant displacement factors equal to zero.

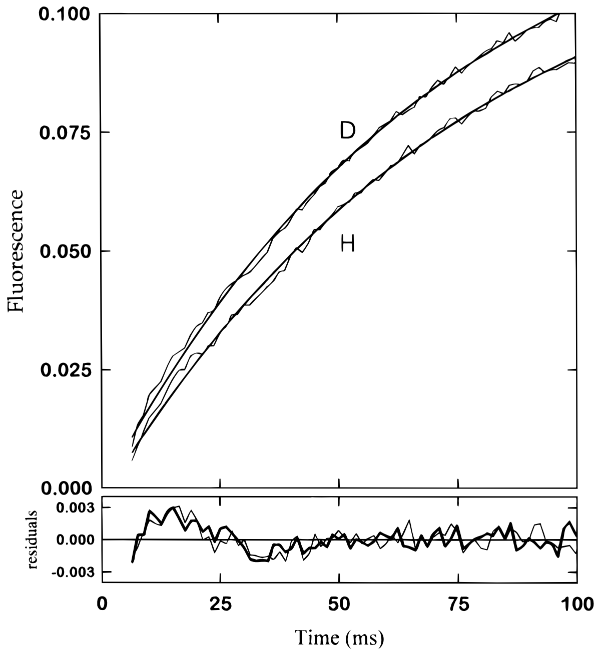

FIGURE 5: The same experiment observed by 340 nm-excited fluorescence.

discarded—the only criterion to be met is that the residuals of the fit be sufficiently small and so distributed that they cannot make kinetically significant contributions to the derivative time courses. The deviations between the data and the fitting function constitute the major source of error in the final KIE curve. The thick lines in Figure 4 (and in Figures 5 and 6) represent the best fits of the data to an equation of the form:[2]

$$f = a_0 + a_1 e^{-k_1 t} + a_2 e^{-k_2 t} \qquad (9)$$

The lower panels in Figures 4−6 represent the fit residual on an expanded scale. It can be seen that they contain deviations which could lead to substantial contributions to the individual $d[s^H]/dt$ and $d[s^D]/dt$ terms of eq 8 (particularly in Figure 5). The extremely close tracking of the respective H and D residual curves, however, shows that these deviations must represent minor flow disturbances rather than chemical events. In any case, their effects are minimized in the $\mathrm{KIE_{obs}}(t)$ function, which represents their quotient.

The $\mathrm{KIE_{obs}}(t)$ for the absorbance data of Figure 4 is shown in curve A of Figure 7. The vertical marks on each curve represent our estimates of the probable error.

In all of the cases presented in this and in the accompanying paper, the deviations between the data and the fitted smoothing function are too small to contribute any significant error to the $\mathrm{KIE_{obs}}$ time courses. The largest source of error here is due to variations in the pipeting between the deuterio-substituted and the unsubstituted reactions. We estimate this error to be no more than 2%. The error bars are calculated by adding and subtracting this amount of $s^H(t)$ and $s^D(t)$ in eqs 5 and 6 and then calculating the upper and lower limits of $\mathrm{KIE_{obs}}$ by applying eqs 5−7.

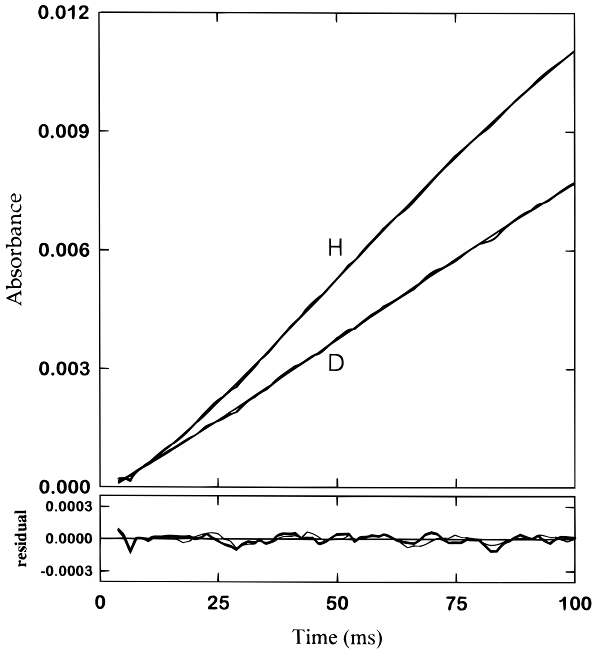

FIGURE 6: The same experiment observed in Figure 4 carried out at pH 6.4.

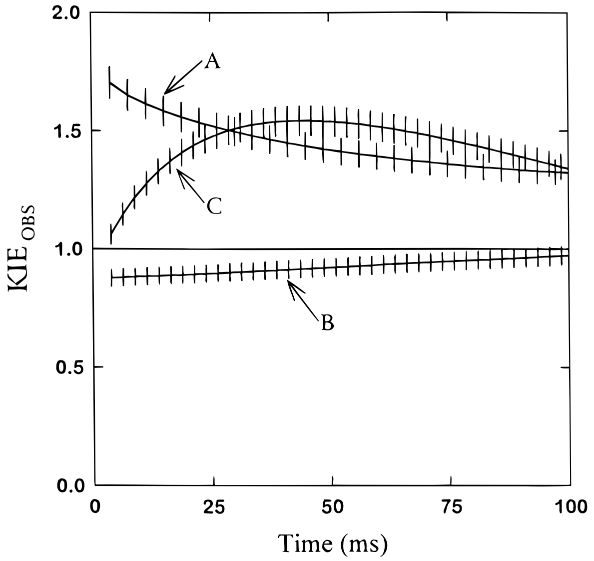

FIGURE 7: $\mathrm{KIE_{obs}}$ values calculated from the data in Figures 4, 5, and 6 shown as A, B, and C, respectively.

Curve A clearly represents the phenomenon we have labeled case I in the theoretical section—there is no significant contribution to this signal from pre-hydride step complexes. $\mathrm{KIE_{int}}$ for this reaction is at least 1.7, but could be higher.[3]

In Figure 5 we show the corresponding results of the identical reaction as observed by 340 nm-excited fluorescence. It is obvious from the raw data traces themselves

---

[2] It should come as no great surprise to find that the early time portion of even a very complex sequential reaction can be fitted very precisely by a general double or even a single exponential function whose parameters have no simple relationship to the actual rate constants of the reaction. This is a reflection of the well-known fact that in a multistep reaction only a single exponential function can be discerned unless the rate constants differ by a factor of 7 or more (Bernasoni, 1976). It is for this reason that relaxation kinetics studies very frequently demonstrate only a single relaxation time even in reactions which are known to involved three or four discrete steps.

[3] The experimental reactions presented here are chosen only to represent the existence of the three phenomenological cases predicted by the theory. We will defer any specific mechanistic interpretations of their behavior until they are presented elsewhere in their appropriate context [as in the accompanying paper (Maniscalco et al., 1996)].

(labeled H and D) that, as observed by this signal, the reaction now shows an *inverse* $\mathrm{KIE}_{\mathrm{obs}}(t)$. The fitting functions (single exponential term forms of eq 9, in this case) are shown by the thick lines in the figure. The resulting $\mathrm{KIE}_{\mathrm{obs}}(t)$ from this experiment is shown as curve B in Figure 7. This result is a clear example of the pattern predicted under case II of the theory described above, where in the initial stages of the reaction time course only *pre*-hydride complex formation is contributing significantly to the signal being observed. (It is presumed that the value of $\mathrm{KIE}_{\mathrm{obs}}(t)$ is unity at $t = 0$ and reaches a value of 0.9 in the instrument dead time.)

In Figure 6, we show the corresponding results of the same reaction, now run at pH 6.4, measured by the 340 nm absorbance signal (as in Figure 4). The data are treated as in Figure 4. The resulting $\mathrm{KIE}_{\mathrm{obs}}(t)$ curve for this experiment is shown by curve C of Figure 7. Again, the residuals shown in the bottom panel of the figure indicate that the deviations from ideality occur equally in both the H and D curves and thus do not contribute to the $\mathrm{KIE}_{\mathrm{obs}}(t)$ curve. The shape of the curve indicates that this absorbance signal contains significant contributions from both pre- and post-hydride complexes and is an example of case III behavior where post-hydride complexes dominate the signal.

We have demonstrated here the fact that the examination of the time and signal dependence of transient-state $\mathrm{KIE}_{\mathrm{obs}}$ functions serves to identify the origin of the specific signals themselves and locate the complexes from which they arise with regard to their pre- or post-hydride step position on the reaction time course. Under certain circumstances they may also establish the value of $\mathrm{KIE}_{\mathrm{int}}$ even in cases where kinetic masking would make such a determination impossible by either techniques. The steady-state KIE approach [particularly using the approaches of Cleland, Cook, and Northrop (Cleland, 1982), employing both deterium and tritium and combining forward and reverse rate measurements] is based on a more elegant mathematical paradigm than the numerically integrated approach here and can provide very useful mechanistic insights. The transient-state approach described here offers some advantages of its own, however. The experiments rely on the comparison of single side-by-side transient time courses, rather than on the concentration dependences of a set of rate measurements. Since late slow steps contribute less to the transient rate, the transient isotope effects themselves are often substantially larger than their steady-state counterparts. Finally, their intrinsic signal dependence offers a very wide range of experimental opportunity, since each optical signal (absorbance, fluorescence, CD, etc.) and each variation in wavelength of such signals potentially provide a differential sensitivity to the various complexes along the reaction time course. The application of this new approach to the assignment of the locations of specific complexes along the reaction coordinate of an enzyme reaction is demonstrated in the accompanying paper (Maniscalco et al., 1996).

ACKNOWLEDGMENT

This paper is dedicated to the memory of my associate of many years, Albert Van Walleghem, who passed away this year.

REFERENCES

Bernasconi, C. F. (1976) *Relaxation Kinetics*, p 144, Academic Press, Orlando, FL.

Cleland, W. W. (1982) *CRC Crit. Rev. Biochem. 13*, 385.

Cleland, W. W. (1989) *Z. Naturforsch. 45*, 445.

Fisher, H. F., Bard, J. R., & Prough, R. A. (1970) *Biochem. Biophys. Res. Commun. 41*, 601.

Maniscalco, S. J., Saha, S. K., Vicedomini, P., & Fisher, H. F. (1996) *Biochemistry 35*, 89−94.

Melander, L., & Sanders, W. H. (1980) in *Reaction Rates of Isotopic Molecules*, John Wiley & Sons, New York.

Moore, J. W., & Pearson, R. G. (1981) in *Kinetics and Mechanism*, John Wiley & Sons, New York.

Saha, S. K., Maniscalco, S. J., Singh, N., & Fisher, H. F. (1994) *J. Biol. Chem. 269*, 29592.

BI9509107